International Journal of Energy
ISSN: 2957-9473 | Vol. 9, No. 2, 2026

Effect of Electrolyte Surface Modification on the Cathode Performance of Solid Oxide Fuel Cells

Zhaotong Wei, Zhiqun Cao *, Hao Dong

Department of Physics, Heilongjiang University of Science and Technology, Harbin, Heilongjiang, 150001, China
*** Corresponding author:** Zhiqun Cao (Email: zqcao2025@163.com)

Abstract: Solid oxide fuel cells (SOFCs) are promising clean energy conversion devices, but their intermediate-temperature performance is severely limited by high polarization resistance, originating from sluggish cathodic oxygen reduction reaction (ORR) kinetics and insufficient electrolyte-cathode interfacial contact. Herein, a homogeneous YSZ rough layer was fabricated on the cathode side of 8 mol% yttria-stabilized zirconia electrolyte via spin-coating. Half-cells with $La_{0.3}Sr_{0.7}Ti_{0.3}Fe_{0.7}O_{3-\delta}$ (LSTF) cathode were assembled, and their electrochemical performance was systematically investigated at 800 °C under 0.05 and 0.21 atm oxygen partial pressure. This modification significantly enlarges the interfacial contact area and extends triple phase boundaries, achieving a maximum 33.4% reduction in polarization resistance at 800 °C under 0.05 atm. The enhancement mainly stems from reduced charge transfer and oxygen adsorption/dissociation resistance, providing a facile low-cost route for intermediate-temperature SOFC cathode optimization.

Keywords: Solid Oxide Fuel Cells; Electrolyte Surface Modification; Oxygen Reduction Reaction; Polarization Resistance.

1. Introduction

The extensive consumption of conventional fossil fuels has led to massive greenhouse gas emissions, exacerbating global climate change and environmental pollution, which poses formidable challenges to the sustainable development of human society and the stability of global ecosystems [1]. Accordingly, the development of high-efficiency, clean energy conversion technologies has become a core research priority to address the global energy and environmental crises. SOFCs, as all-solid-state electrochemical devices that directly convert the chemical energy of fuels into electrical energy, have been widely recognized as one of the most promising alternatives to conventional fossil fuel-based power generation systems, owing to their ultra-high energy conversion efficiency and significantly reduced carbon dioxide emissions. However, to extend the service life of SOFC systems and promote their large-scale commercialization, further in-depth investigations on the performance optimization of electrode and electrolyte materials, as well as the innovation of fabrication processes, are still urgently required [2,3].

A typical SOFC consists of three core components: a cathode, an electrolyte, and an anode. Specifically, the cathode is responsible for the reduction of oxygen to oxygen ions; the electrolyte serves as the dense membrane for oxygen ion transport; and the anode is the reaction site where fuel oxidation occurs with the release of electrons [4]. The electrons are subsequently transported to the cathode through an external circuit, completing the entire electrical energy output cycle. Under intermediate-to-low temperature conditions (700–850 °C), the performance improvement of SOFCs is generally limited by the sluggish kinetics of the cathodic ORR, while the interfacial contact state between the electrolyte and cathode is a critical factor determining the ORR efficiency [5]. Conventional flat electrolyte surfaces have a limited contact area with the cathode, resulting in an insufficient length of TPBs, which in turn increases the polarization resistance and restricts the overall electrochemical performance of the cell [6.7]. This constitutes the core motivation of this work, which aims to optimize the interfacial contact and boost the cathodic performance of SOFCs via electrolyte surface modification.

To date, most studies on SOFC performance optimization have focused on electrode material modification or operating condition regulation. In contrast, the strategy of optimizing the interfacial microstructure through electrolyte surface modification has attracted increasing attention due to its facile operation, low cost, and direct effectiveness. Yttria-stabilized zirconia (YSZ) is the dominant material for SOFC electrolytes, owing to its excellent chemical stability and high oxygen ionic conductivity [8]. LSTF, as a typical mixed ionic-electronic conductor, possesses a thermal expansion coefficient well-matched with YSZ and stable ORR catalytic activity, making it a promising cathode candidate for intermediate-to-low temperature SOFCs [9,10]. However, in existing reports, although heterogeneous material modification layers can improve interfacial performance, they may trigger interfacial heterogeneous reactions to form high-impedance secondary phases, which is detrimental to the long-term operational stability of SOFCs [11-13].

On this basis, this work innovatively adopted a homogeneous material modification strategy. A YSZ rough layer was fabricated on the cathode side of the YSZ electrolyte via a spin-coating method to construct two electrolyte substrates with distinct surface roughness (the unmodified pristine sample is denoted as YSZ-S, and the spin-coated modified sample is denoted as YSZ-R). Half-cells were then assembled with LSTF as the cathode material. Within the intermediate-to-low temperature range of 700–850 °C, by adjusting the cathode oxygen partial pressure (pO_2: 0.05 atm, 0.09 atm, 0.13 atm, 0.17 atm, and 0.21 atm) in combination with electrochemical impedance spectroscopy (EIS) analysis, we investigated the influence law and underlying mechanism of electrolyte surface roughness on the electrochemical performance of the cells. This work provides a facile and feasible technical route for the cathodic performance optimization of intermediate-temperature

SOFCs.

2. Experimental

2.1. Materials and Preparation

The electrode material $La_{0.3}Sr_{0.7}Ti_{0.3}Fe_{0.7}O_{3-\delta}$ was prepared by the sol-gel method. $La(NO_3)_3{\cdot}6H_2O$, $Sr(NO_3)_2$, $Fe(NO_3)_3{\cdot}9H_2O$ and $C_{16}H_{36}O_4Ti$ were weighed according to the stoichiometric ratio, added into deionized water in sequence, then the beaker was placed on a magnetic stirrer and stirred evenly at a rotation speed of 400 r/min.

Subsequently, citric acid and ethylenediaminetetraacetic acid (EDTA) were added to the above mixed solution at a molar ratio of total metal ions: citric acid: EDTA = 1:1:2, and stirred until complete dissolution. The pH of the solution was adjusted to 7.0 by slow dropwise addition of aqueous ammonia, during which the solution turned purplish-red. The resulting solution was transferred to a thermostatic water bath at 90 °C, and stirred continuously at 300 rpm with a digital constant-speed high-torque electric stirrer until a purplish-brown colloid was formed.

The as-prepared wet gel was transferred to an oven and heated at 200 °C for 12 h to evaporate residual moisture and form a dry gel, during which the sample expanded and turned brown in the oven. The dry gel was collected and ground for 2 h to obtain the precursor powder. The ground precursor powder was mixed with anhydrous ethanol at an equal mass ratio, followed by combustion to remove partial organic components. The powder after combustion was further ground for 2 h, and finally calcined in a muffle furnace at 1100 °C for 4 h to acquire the final LSTF cathode powder. The phase purity and microstructure of the as-synthesized cathode material are presented in Fig. 1.

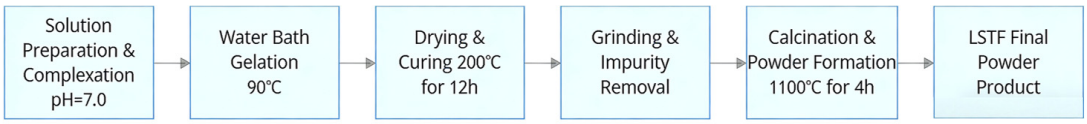

Fig 1. Flow Chart for the Fabrication of $La_{0.3}Sr_{0.7}Ti_{0.3}Fe_{0.7}O_{3-\delta}$ Electrode

2.2. Electrolyte Surface Modification

To address the performance bottlenecks of electrolytes fabricated via the conventional dry pressing method, this work innovatively proposed a spin-coating modification strategy. A YSZ rough layer was spin-cathode coated on the surface of the YSZ electrolyte to obtain electrolyte pellets with a single-side roughened surface. The fabrication and surface modification process of the YSZ electrolyte are illustrated in Fig. 2.

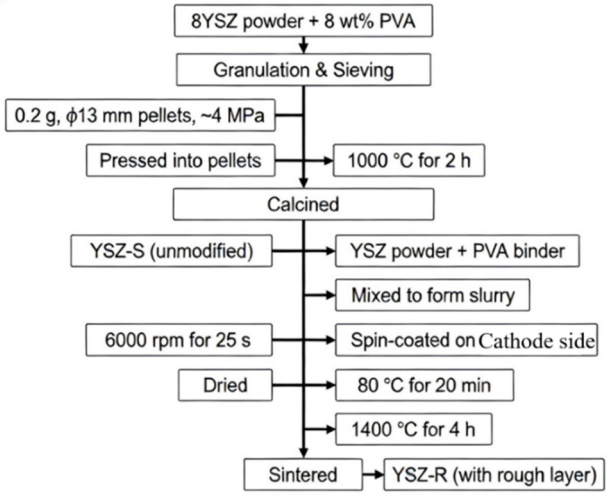

Fig 2. Schematic Illustration of the YSZ Electrolyte Surface Modification Proces

To ensure the comparability of all samples, the weight of the electrolyte green bodies was uniformly controlled at 0.2 g. 8YSZ powder was mixed with 8 wt% polyvinyl alcohol (PVA, used as a binder) for granulation, followed by sieving. 0.2 g of the as-granulated powder was uniaxially pressed into green pellets using a 13 mm diameter steel die under a pressure of ~4 MPa, and subsequently calcined at 1000 °C for 2 h to obtain dense 8YSZ electrolyte pellets with a diameter of 13 mm. Afterwards, YSZ powder was mixed with the organic binder PVA at a specific ratio to prepare the slurry for the YSZ rough layer. The slurry was spin-coated on the cathode side of the electrolyte pellets using a spin coater with a fixed parameter of 6000 rpm for 25 s. After drying at 80 °C for 20 min, the modified electrolyte pellets were sintered at 1400 °C for 4 h, finally yielding the electrolyte pellets integrated with a rough layer. Two sets of electrolyte samples were prepared in this work: the unmodified pristine sample was denoted as YSZ-S, and the modified sample with the roughened layer was designated as YSZ-R.

3. Results and Discussion

3.1. Surface Microstructure of Electrolytes with Different Surface Modifications

Fig. 3 presents the scanning electron microscopy (SEM) images of the surface and cross-sectional microstructure of the as-prepared YSZ electrolytes. The pristine YSZ-S sample exhibits a relatively smooth surface, while the modified YSZ-R sample shows a distinct rugged and undulating structure with significantly enhanced surface roughness. Obvious large particle agglomeration, alternating peak-valley features, and a wide particle size distribution are observed on the surface of YSZ-R.

This structure effectively enlarges the interfacial contact area between the cathode and electrolyte, extends the effective length of the TPBs, and provides more abundant active sites for the ORR. It further enhances the charge transfer efficiency at the electrode-electrolyte interface, thus achieving a remarkable optimization of the overall electrochemical performance of the cell.

3.2. Electrochemical Performance Analysis

Fig. 4 presents the EIS Nyquist plots of the cells, measured at 800 °C with the oxygen partial pressure (pO_2) regulated from 0.05 atm and 0.21 atm by continuously feeding a mixed gas of O_2 and N_2 to the cathode side throughout the test. It can be observed from the plots that all EIS patterns obtained at the same temperature exhibit a consistent variation trend, and each consists of two well-defined semicircles. The high-frequency intercept on the real axis (Z') corresponds to the

ohmic resistance (R_0).

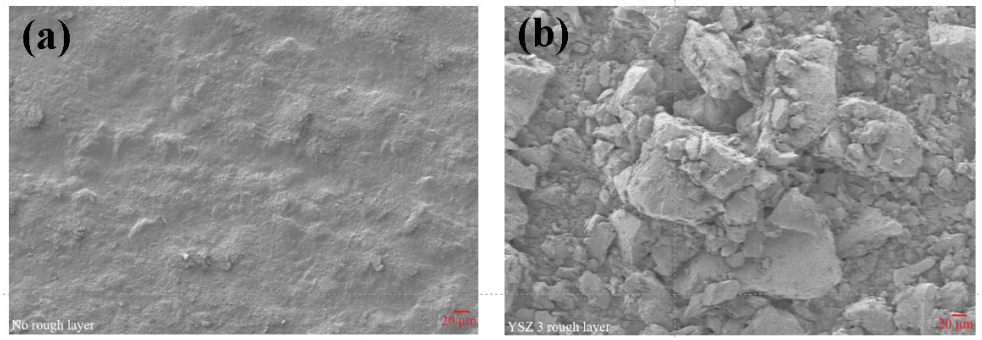

Fig 3. SEM images of the surfaces for the YSZ-S (a) and YSZ-R (b) electrolyte films

This value remains nearly unchanged under all test conditions and maintains at a low level overall, indicating that the ohmic resistance is not affected by the fluctuation of pO_2, which is in good agreement with previously reported results. The ohmic resistance is mainly derived from the voltage drop across components including the electrolyte, conducting wires, and interconnects, and its value is dominantly determined by the oxygen ionic conductivity and thickness of the electrolyte. The two semicircles in the Nyquist plots correspond to the polarization resistance (R_p), which includes the contributions from both activation polarization and concentration polarization, and is closely associated with processes such as the electrochemical reaction on the electrode surface, as well as the adsorption and dissociation of oxygen species. With the increase of pO_2, the total polarization resistance shows a significant downward trend, and the impedance values corresponding to both the high-frequency and low-frequency arcs decrease to varying degrees. This indicates that the rate-determining steps (RDS) corresponding to the two semicircles are both affected by the oxygen partial pressure. Notably, the morphology of the high-frequency and low-frequency arcs in the EIS plots varies at different temperatures, which demonstrates that the change in temperature can alter the RDS of the electrochemical reactions in the cell. In addition, the regulation effect of pO_2 on the polarization resistance shows slight differences at different temperatures. At lower temperatures, the increase in polarization resistance induced by low pO_2 is more pronounced, which is mainly attributed to the intrinsically sluggis

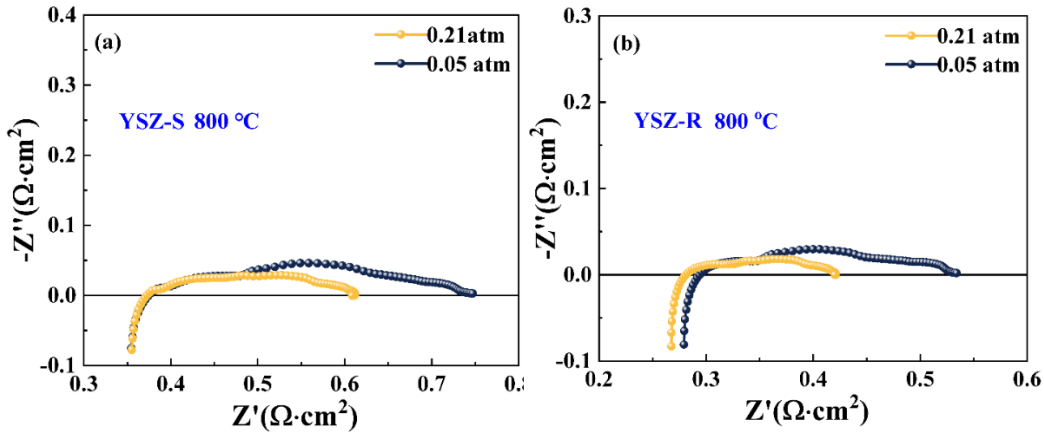

Fig 4. The Electrochemical impedance spectroscopy Nyquist curves of YSZ-S based half-cells at (a) 800 °C , and YSZ-R based half-cells at (b) 800 °C, under oxygen partial pressures ranging from 0.21 atm and 0.05 atm

Table 1. Comparison of Polarization Resistance of YSZ-S and YSZ-R under Different Oxygen Partial Pressures at 800 °C

PO_2(atm)	YSZ-S (R Ω cm^2)	YSZ-R (R Ω cm^2)
0.05	0.39	0.26
0.21	0.25	0.16

4. Conclusion

To address the key bottlenecks of IT-SOFCs, namely the high polarization resistance caused by the sluggish cathodic ORR kinetics and insufficient interfacial contact between the electrolyte and cathode, in this work, we fabricated a YSZ rough layer on the cathode side of YSZ electrolytes via a spin-coating technique. Two electrolyte substrates with distinct surface structures were constructed: the unmodified pristine sample YSZ-S and the surface-modified sample YSZ-R. Half-cells were assembled with LSTF as the cathode, and the effects of electrolyte surface modification on the electrochemical performance of SOFCs were systematically investigated in the intermediate-to-low temperature range of 700–850 °C under pO_2 of 0.05–0.21 atm. The spin-coating technique markedly increases the surface roughness of the electrolyte, enlarges the interfacial contact area between the LSTF cathode and electrolyte, and extends the effective length of TPBs. Meanwhile, the LSTF cathode exhibits excellent chemical compatibility with the YSZ electrolyte at the sintering temperature adopted in this work, with no undesired secondary reaction phases formed. Electrochemical measurements demonstrate that both pO_2 and surface roughness impose significant impacts on the polarization resistance (R_p): the polarization resistance decreases with the

increase of pO_2. Under identical operating conditions, the R_p of YSZ-R is significantly lower than that of YSZ-S, with a maximum reduction of 54.2% achieved at 800 °C under a pO_2 of 0.05 atm, and the performance enhancement is more pronounced under low-temperature and low-pO_2 conditions. The electrolyte surface modification optimizes the cell performance mainly by reducing the charge transfer resistance and the oxygen adsorption/dissociation resistance, while it exerts a negligible effect on the oxygen ion diffusion resistance. This homogeneous YSZ spin-coating modification strategy is facile and low-cost, and effectively avoids the interfacial compatibility issues caused by heterogeneous material modification. It provides a feasible and effective technical route for the cathodic performance optimization of intermediate-to-low temperature SOFCs, and possesses important guiding significance for promoting the commercial application of SOFCs.

References

[1] Ding Dong, Li Xiaxi, Lai Samson Yuxiu, Gerdes Kirk, Liu Meilin. Enhancing Sofc Cathode Performance by Surface Modification Through Infiltration [J]. Energy & Environmental Science, 2014,7 (2): 552-575.

[2] Juhl Mette, Primdahl Soren, Manon Carrie, Mogensen MogensBjerg. Performance/structure correlation for composite SOFC cathodes [J]. Journal of Power Sources, 1996, 61 (1-2): 173-181.

[3] Kong Wei, Han Zhen, Lu Siyu, Gao xiang, Wang Xiaorong. A novel interconnector design of SOFC [J]. International Journal of Hydrogen Energy, 2020, 45 (39): 20329-20338.

[4] Ding Dong, Liu Mingfei, Liu Zhangbo, LiXiaxi, Blinn Kevins, Zhu Xingbao, LiuMinlin. Efficient electro-catalysts for enhancing surface activity and stability of SOFC cathodes [J]. Advanced Energy Materials, 2013, 3 (9): 1149-1154.

[5] Xia Baixia, Zhang Hanxia, Yao Chuangang, Louhao, Chen Mingcun, Zhang zhe, Sun Yuxi, Zhang Wenwen, Wang Haocong, Liang Xiaoshi, Cai Kedi. Enhancing ORR activity and CO_2 tolerance of $Pr_{0.4}Sr_{0.6}Co_{0.2}Fe_{0.8}O_{3-\delta}$-based SOFC cathode through synergistic doping and surface modification [J]. Applied Surface Science, 2024, 649: 159143.

[6] Ge Xiaoming, Fu Changjing, Chan Siew Hwa. Three phase boundaries and electrochemically active zones of lanthanum strontium vanadate–yttria-stabilized zirconia anodes in solid oxide fuel cells [J]. Electrochimica acta, 2011, 56 (17): 5947-5953.

[7] Wang Rongtsu, Chang Hrongyi, Wang Jungchang. An Overview on the Novel Core-Shell Electrodes for Solid Oxide Fuel Cell (SOFC) Using Polymeric Methodology [J]. Polymers, 2021, 13 (16): 2774.

[8] Jung Inyong, Lee Daehee, Lee Seong Oh, Kim Dongha, Moon Jooho. LSCM–YSZ nanocomposites for a high performance SOFC anode [J]. Ceramics International, 2013, 39 (8): 9753-9758.

[9] Deseure eseure, Bultel Y, Dessemond L, Siebert Elisabeth. Theoretical optimisation of a SOFC composite cathode [J]. Electrochimica Acta, 2005, 50 (10): 2037-2046.

[10] Chen Sigeng, Zhang Hzixia, Yao Chuangang, Lou Hao, Chen Mingcun, Liang Xiaoshi, Cai Kedi. Review of SOFC cathode performance enhancement by surface modifications: recent advances and future directions [J]. Energy & Fuels, 2023, 37 (5): 3470-3487.

[11] Lu Fei, Yang Mengjie, Wu Changhui,Jia Xusheng, He Hao, Chao Mingjv, Cai Bin. Application of a negative thermal expansion oxide in SOFC cathode [J]. Ceramics International, 2021, 47 (1): 1095-1100.

[12] Cascos V, Martínez-Coronado R, Alonso Joseantonin. Structural and electrical characterization of the Co-doped $Ca_2Fe_2O_5$ brownmillerite: Evaluation as SOFC-cathode materials [J]. International Journal of Hydrogen Energy, 2015, 40 (15): 5456-5468.

[13] Li Huan, Sun Liping, Li Qiang, Zhao Hui, Huo Lihua, Bassat JeanMarc, Roughier Aline, Fourcade Sebastien. Electrochemical performance of double perovskite Pr_2NiMnO_6 as a potential IT-SOFC cathode[J]. International journal of hydrogen energy, 2015, 40 (37): 12761-12769.